

Full length article

Oxygen nonstoichiometry, defect equilibria, and thermodynamic characterization of LaMnO₃ perovskites with Ca/Sr A-site and Al B-site doping

M. Takacs^a, M. Hoes^a, M. Caduff^a, T. Cooper^a, J.R. Scheffe^{b,*}, A. Steinfeld^{a,*}^a Department of Mechanical and Process Engineering, ETH Zurich, 8092 Zurich, Switzerland^b Department of Mechanical and Aerospace Engineering, University of Florida, Gainesville, FL 32611-6250, USA

ARTICLE INFO

Article history:

Received 24 August 2015

Received in revised form

14 October 2015

Accepted 16 October 2015

Available online xxx

Keywords:

Solar fuels

Perovskites

Oxygen nonstoichiometry

Thermochemical

Defect chemistry

ABSTRACT

This work encompasses the thermodynamic characterization of four doped lanthanum manganites, namely La_{0.6}A_{0.4}Mn_{1-y}Al_yO₃ (A = Ca, Sr and y = 0, 0.4), all showed to be promising redox materials for the solar thermochemical splitting of H₂O and CO₂ to H₂ and CO. We present oxygen nonstoichiometry measurements in the temperature range $T = 1573\text{ K} - 1773\text{ K}$ and oxygen partial pressure range $p_{\text{O}_2} = 4.5066 \times 10^{-2}\text{ bar} - 9.9 \times 10^{-5}\text{ bar}$. For a given T and p_{O_2} , oxygen nonstoichiometry is found to be higher when replacing the divalent dopant Sr in La_{0.6}Sr_{0.4}MnO₃ by the divalent Ca but also increases significantly when additionally doping 40 mol-% Al to the Mn-site. La_{0.6}Ca_{0.4}Mn_{0.6}Al_{0.4}O₃ revealed the highest mass specific oxygen release, 0.290 mol O₂ per kg metal oxide at $T = 1773\text{ K}$ and $p_{\text{O}_2} = 2.360 \times 10^{-3}\text{ bar}$ and 0.039 mol kg^{-1} at $T = 1573\text{ K}$ and $p_{\text{O}_2} = 4.5066 \times 10^{-2}\text{ bar}$. It is shown that the chemical defect equilibrium of all four perovskites can be accurately described by the two simultaneous redox couples Mn⁴⁺/Mn³⁺ and Mn³⁺/Mn²⁺. Thermodynamic properties, namely partial molar enthalpy, entropy and Gibbs free energy are consequently extracted from the defect models. Partial molar enthalpy decreases with increasing oxygen nonstoichiometry for the Al-doped perovskites whereas the opposite trend is observed for the others. The enthalpy falls within the range 260–300 kJ mol⁻¹ for all the materials. Equilibrium hydrogen yields upon oxidation with H₂O are determined as a function of redox conditions. Although reduction extents of the perovskites are greater compared to CeO₂, oxidation with H₂O and CO₂ is thermodynamically less favorable. This leads to lower mass specific fuel productivity compared to CeO₂ under most conditions relevant for solar thermochemical cycles.

© 2015 Acta Materialia Inc. Published by Elsevier Ltd. All rights reserved.

1. Introduction

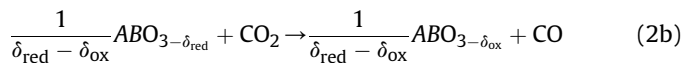
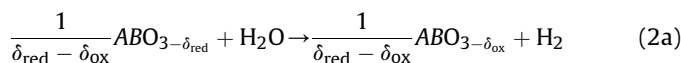
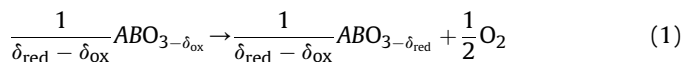
Nonstoichiometric ceria (CeO₂) is currently considered to be a state-of-the-art redox material for solar-thermochemical splitting of H₂O and CO₂ to H₂ and CO (syngas) because of its rapid oxidation and reduction kinetics and its morphological stability over a range of temperatures and reduction extents [1]. Compared to other metal oxide systems (e.g. volatile ZnO [2] and non-volatile ferrites [3,4]), ceria shows relatively low fuel productivity per unit mass of metal oxide [5–7]. It has been shown that reduction extents of ceria can be increased by introducing 4+ valence dopants such as Zr⁴⁺ [8–12] and Hf⁴⁺ [8,13] into the ceria lattice. However,

thermodynamic calculations for Zr⁴⁺-doped ceria [7,12] showed that oxidation with H₂O is less favorable compared to pure ceria. This results in a lower theoretical solar-to-fuel energy conversion efficiency for Zr⁴⁺-doped ceria because of larger temperature swings between the redox steps and/or excess oxidant gas [7]. Lower conversion efficiency was also reported for other ceria dopants such as Gd³⁺, Y³⁺, Sm³⁺, Ca²⁺ and Sr²⁺ [6].

Perovskite oxides have recently been proposed as promising alternative reactive intermediates for solar thermochemical H₂O/CO₂ splitting because of potentially increasing the energy conversion efficiency by lowering the reduction temperature or increasing the mass specific fuel yield [14–23]. The two-step solar-thermochemical cycle based on a generic perovskite (ABO₃) is represented by

* Corresponding authors.

E-mail addresses: jscheffe@ufl.edu (J.R. Scheffe), aldo.steinfeld@ethz.ch (A. Steinfeld).



where Eq. (1) represents the high-temperature endothermic reduction and Eq. (2) the lower temperature exothermic oxidation with H₂O (a) and CO₂ (b). δ_{red} and δ_{ox} represent the oxygen nonstoichiometry after reduction and oxidation, respectively, whereas the difference $\delta_{\text{red}} - \delta_{\text{ox}}$ is the molar amount of fuel produced per mole of metal oxide. Scheffe et al. [14] considered strontium-doped lanthanum manganites La_{1-x}Sr_xMnO₃ ($x = 0.30, 0.35, 0.40$) and reported reduction extents of La_{0.6}Sr_{0.4}MnO₃ to be nearly 6.5 times larger than those of ceria at 1600 K and twice larger at 1800 K, both for $p_{\text{O}_2} = 10^{-5}$ bar. However, it was shown that their theoretical solar-to-fuel energy conversion efficiency is lower compared to that of ceria because of the thermodynamically less favorable oxidation with CO₂ and H₂O. Based on measurements of Mizusaki et al. [15], Yang et al. [16] concluded higher reduction extents and, consequently, higher fuel yields with increasing x for La_{1-x}Sr_xMnO₃ ($0 \leq x \leq 0.5$), while H₂O-to-H₂ conversion rate decreased with increasing x . This led to the conclusion that intermediate doping levels may be optimal for solar-to-fuel energy conversion. McDaniel et al. [17] showed even higher CO and H₂ yields when additionally doping Al to the B-site of La_{1-x}Sr_xMnO₃ while maintaining fast oxidation rates with CO₂ and H₂O. Dey et al. [18] showed increasing reduction extents and fuel productivity when replacing the divalent A-site dopant Sr in La_{1-x}Sr_xMnO₃ with Ca and obtained best results for $x = 0.5$. In another recent work [19], they investigated two series of perovskite oxides, Ln_{0.5}Sr_{0.5}MnO₃ and Ln_{0.5}Ca_{0.5}MnO₃ (Ln = La, Nd, Sm, Gd, Dy, and Y) and concluded highest O₂ release for the manganite with the smallest A-site cation radius (in this case Y). A comparison between La_xSr_{1-x}MO₃ (M = Mn, Co, Fe) and Ba_xSr_{1-x}(Co,Fe)O₃ [20] showed best results for the Mn-containing perovskites. In a very recent study by Cooper et al. [21], Sr and Ca A-site doped lanthanum-manganites, with and without B-site doping of Al, were examined for redox performance and compared to the state-of-the-art material ceria. La_{0.6}Sr_{0.4}Mn_{0.6}Al_{0.4}O₃ and La_{0.6}Ca_{0.4}Mn_{0.6}Al_{0.4}O₃ reach four to nine times higher reduction extents compared to ceria in the temperature range $T = 1473 \text{ K} - 1673 \text{ K}$, while maintaining fast oxidation kinetics with CO₂. Bork et al. [22] reported that La_{0.6}Sr_{0.4}Cr_{1-x}Co_xO₃ with the optimal dopant concentration $x = 0.2$ can split up to 25 times more CO₂ when cycling at $T = 1073 \text{ K} - 1473 \text{ K}$ compared to ceria or exhibits similar reduction extents ($\delta = 0.034$) at 300 K lower temperatures (1473 K instead of 1773 K). On the other hand, cyclability redox studies by Galvez et al. [23] revealed that the chemical stability of Ca, Sr and Al-doped La–Mn perovskites is detrimentally affected by sintering and by the formation and eventual segregation of a carbonate phase during oxidation by CO₂.

Some of the conclusions drawn for the perovskites discussed above are mainly based on qualitative reduction experiments under an inert flow of low p_{O_2} and oxidation under a relatively high flow of CO₂ and/or H₂O in a thermogravimetric analyzer [18–20,22] and/or in an electrically heated furnace coupled to a gas analysis [17,18]. Such experiments with large excess of CO₂ and/or H₂O can result in misleading conclusions, as indicated by various thermodynamic analyses [14,16,21]. In the work of Yang et al. [16], the amount of H₂O needed to oxidize La_{1-x}Sr_xMnO₃ ($0 \leq x \leq 0.4$) to a certain δ_{ox} ,

and hence produce a fixed amount of H₂ in a closed system with variable volume was calculated from thermodynamic data. Similar calculations were performed by Scheffe et al. [14] and Cooper et al. [21], however, there, the initial amount of CO₂ and/or H₂O was fixed and the fuel yield was predicted as a function of oxidation temperature. Such thermodynamic fuel yield calculations allow for an accurate determination of the material's potential to efficiently split CO₂ and/or H₂O.

In this work, we build on the recent work of Cooper et al. [21] and report detailed oxygen nonstoichiometry measurements of La_{0.6}A_{0.4}Mn_{1-y}Al_yO₃ ($A = \text{Ca, Sr}$ and $y = 0, 0.4$) over a wide temperature range $T = 1573 \text{ K} - 1773 \text{ K}$ and oxygen partial pressure range $p_{\text{O}_2} = 4.5066 \times 10^{-2} \text{ bar} - 9.9 \times 10^{-5} \text{ bar}$. The refinement of the nonstoichiometry measurements allows the development of more appropriate defect models to describe the defect chemical equilibria and to extract finer trends in partial molar thermodynamic properties ($\Delta \bar{h}_\text{O}^\circ$, $\Delta \bar{s}_\text{O}^\circ$, $\Delta \bar{g}_\text{O}^\circ$). From such data we determine equilibrium hydrogen yields and evaluate the potential of these lanthanum-manganites to be used as reactive intermediates in solar thermochemical redox cycles.

2. Experimental section

2.1. Sample preparation and characterization

La_{0.6}Sr_{0.4}MnO₃ (LSM40), La_{0.6}Ca_{0.4}MnO₃ (LCM40), La_{0.6}Sr_{0.4}Mn_{0.6}Al_{0.4}O₃ (LSMA) and La_{0.6}Ca_{0.4}Mn_{0.6}Al_{0.4}O₃ (LCMA) perovskite powders were synthesized by sol–gel method as described by Scheffe et al. [8]. The corresponding metal nitrates (see Table 1 in electronic supplementary information¹ (ESI)) and anhydrous citric acid (Sigma–Aldrich, catalog nr. 251275) in aqueous solution were used to carry out the synthesis. The ratio of the metal cations to the citric acid was 1:1.5. The aqueous solution was slowly heated up to 573 K to perform the pyrolysis. Afterwards, powders were calcined at 1273 K under air for 5 h. Dense cylindrical pellets were obtained by uniaxially cold-pressing the powder at 5 tons followed by sintering at 1773 K under air atmosphere for 24 h. The approximate dimensions after sintering were 6.4–6.9 mm diameter and 1–2 mm height and the mass of the pellets was ~250 mg (LSM40), ~290 mg (LCM40), ~150 mg (LSMA) and ~270 mg (LCMA). Dopant concentrations were measured by inductively coupled plasma-atomic emission spectroscopy (ICP-OES) and deviated by less than 4% from their nominal composition for LSMA and LCMA. Powder X-ray diffraction (XRD) was performed in the Bragg Brentano geometry using Cu K α radiation (Philips, PANalytical/X'Pert MPD/DY636, $\lambda = 1.5406 \text{ \AA}$, $2\theta = 20 - 100^\circ$, $0.01^\circ \text{ s}^{-1}$ scan rate, 45 kV/20 mA output). Scanning electron microscopy (SEM) of the dense pellets was conducted on a TM-1000Microscope (Hitachi, 15 kV accelerating voltage). ICP-OES analysis, XRD patterns and SEM images are shown in ESI.

2.2. Thermal analysis

Oxygen nonstoichiometry was measured using a thermogravimetric analyzer (TGA, Setaram Setsys Evolution). Pellets were suspended to the balance with a custom-made platinum hook to ensure good exposure to the purge gas and eliminate gas diffusion limitations. The p_{O_2} of the sweep gas was controlled by mixing Ar (Messer, Argon 4.6) with O₂/Ar mixtures (Messer, 5% O₂ 5.0 in Ar 5.0 and 0.1% O₂ 5.0 in Ar 5.0). Gases were mixed with electronic mass

¹ Electronic supplementary information (ESI) available: List of metal nitrates used for sample preparation, ICP-OES analysis, XRD patterns, SEM images, detailed derivation of defect model and additional results.

Download English Version:

<https://daneshyari.com/en/article/7879566>

Download Persian Version:

<https://daneshyari.com/article/7879566>

[Daneshyari.com](https://daneshyari.com)